

High-temperature mechanical behavior of carbon–silicide–carbide composites developed by alloyed melt infiltration

Mohammad Esfahanian^{a,*}, Jens Guenster^a, Juergen G. Heinrich^a,
Juergen Horvath^b, Dietmar Koch^b, Georg Grathwohl^b

^a *Clausthal University of Technology, Institute for Non-metallic Materials, 38678 Clausthal-Zellerfeld, Germany*

^b *Ceramic Materials and Components, University of Bremen, IW3, D-28359 Bremen, Germany*

Received 4 June 2007; received in revised form 20 September 2007; accepted 30 September 2007

Available online 28 November 2007

Abstract

In order to improve high-temperature mechanical properties of silicon-infiltrated SiC materials infiltration with a Si–Ti–MoSi₂ alloyed melt and reinforcement with carbon fibers were investigated. Microstructure, bending strength, and creep resistance of alloy-infiltrated samples with and without reinforcement were studied and compared with silicon-infiltrated samples. The composites reinforced with high-modulus carbon fibers had generally higher bending strengths and lower creep deformations than infiltrated felts. The alloy-infiltrated felts showed more resistance against creep deformation than silicon-infiltrated felts and had higher strengths both at room and at high temperature. Alloy-infiltrated and silicon-infiltrated reinforced composites behaved almost the same at low and high temperatures.

© 2007 Elsevier Ltd. All rights reserved.

Keywords: Composites; Carbon; SiC; Silicides; Infiltration

1. Introduction

Siliconized silicon carbide (SiSiC) can be produced by a melt infiltration process as first proposed by Hillig et al.,^{1,2} whereby a melt infiltrates a porous preform by capillary forces. Advantages such as high density of the final composites, good dimensional precision, and short production times, allow this method to be used in fabricating of heat engine components.³ However, the working temperature of SiSiC ceramics is limited by the softening of residual silicon in the microstructure.^{4–6} To overcome this problem, a silicon-containing alloyed melt can be infiltrated into the preforms. This can result in elimination of residual silicon and consequently in an improved mechanical behavior above 1400 °C.^{7–10} Elements of this alloy form high-temperature resistant silicides and carbides through reactions with carbon and silicon. Molybdenum is a favored element because it reacts with silicon to form MoSi₂, which possesses excellent high-temperature characteristics, a high melting

point, and high resistance against oxidation.¹¹ It shows significant metal-like ductility at high temperatures due to its brittle-to-ductile transition around 900–1000 °C. It is believed that MoSi₂ can improve the fracture toughness of the infiltrated SiC materials.^{12–14} However, temperatures of at least 2100 °C are necessary to infiltrate a material with this substance. This melting temperature can be reduced by addition of silicon and other substances, such as titanium, which has been proven earlier as a suitable choice, regarding high-temperature and oxidation behavior of the composite.⁸ As well as using an alloyed melt for infiltration, reinforcement of infiltrated composites with carbon fibers can also improve their mechanical properties. Especially for composites in which the fibers control the mechanical properties, it is possible to improve the high-temperature mechanical properties through using preforms with high volume fraction of fibers. For this purpose it is necessary to have a moderately bonded fiber–matrix interface which is usually satisfied by coating the fibers with layered-structure materials such as pyrolytic carbon.^{15,16}

In a previous work, development of carbon–silicide–carbide composites free of residual silicon through infiltration of C_f/C preforms and C_f-felts by an alloyed melt was described and also an effective infiltration method was elaborated.^{17,18} This paper

* Corresponding author at: Institute of Ceramics in Mechanical Engineering, University of Karlsruhe, Karlsruhe 76131, Germany. Tel.: +49 721 6087917; fax: +49 721 6088891.

E-mail address: m.esfahanian@yahoo.com (M. Esfahanian).

Table 1
Physical properties of the carbon fiber preforms used for infiltration

Preform	Fiber orientation (°)	Density (g/cm ³)	Thermal expansion coefficient (K ⁻¹)	Thermal conductivity (W/mK)	Porosity (%)
CF222 (C/C)	0/90	1.6–1.65	$0.8\text{--}1.2 \times 10^{-6}$	5 _⊥ , 20–40	6–8
FU-2954 (Felt)	Random	0.13–0.15	2.6×10^{-6}	0.3	40–42

addresses the microstructure and high-temperature mechanical properties of these composites. The high-temperature bending strength and creep resistance of the samples with and without carbon fiber reinforcement are studied. The results are compared with the results obtained for samples infiltrated with pure silicon.

2. Experimental procedure

Two types of carbon preforms (CF222 and FU-2954, Schunk Kohlenstoff GmbH, Giessen, Germany) were infiltrated. The CF222 (C/C-Preform), included several fiber bundles in an amorphous carbon matrix. The fibers were coated with a 100 nm pyrolytic-C layer to ensure a moderately bonded interface and to prevent a heavy reaction between the fibers and silicon below 1600 °C. Between the bundles there were large capillary pores remained from pyrolysis of the matrix. Some of the physical properties of C/C preforms are listed in Table 1. The structure of the C/C preforms is shown in Fig. 1. The FU-2954 (felt) did not include any matrix. The fibers in this preform were not coated and could react with the melt at their surfaces. This preform had no preferred fiber orientation but a much higher porosity in comparison to C/C composites (Fig. 2), so that the infiltrated phases can contribute more to the final mechanical properties.

The chemical composition of Si: 50%, Ti: 14% and MoSi₂: 36% was selected for the infiltrating mixture in this study (MoSiTi alloy). For this mixture, MoSi₂ powder (99.5%, Alfa Aesar, Karlsruhe, Germany) was mixed with Ti (99.4% Alfa Aesar, Karlsruhe, Germany) and Si (99%, Wacker Chemie, Burghausen, Germany). Long beams (8 mm × 8 mm × 120 mm) from each preform were infiltrated with the selected mixture. The infiltration process was performed in a reactor which was

heated by an induction tube furnace. In this reactor the preform could be kept away from the infiltrants until they are completely molten and become an infiltrating alloy. An advantage of this method was the possibility of processing composites without residual silicon at temperatures below 1600 °C which is quite difficult to achieve by other conventional methods. A detailed description of the infiltration process can be found in refs. 17,18

The phase composition and microstructure of the alloy-infiltrated samples were investigated using SEM (Camscan Cs-4, Waterbeach, U.K.) analysis. Mechanical properties of alloy-infiltrated and also silicon-infiltrated samples were measured using universal testing machine (Zwick 1474, Ulm, Germany) equipped with a graphite furnace. The loading span was 25 mm and radius of supporting rolls was 5 mm. Alloy- and silicon-infiltrated samples with and without reinforcement were cut, using a diamond cutting blade, to form 30 mm × 5 mm × 5 mm bending specimens. The specimen's surfaces were polished to achieve a surface roughness less than 0.1 mm. The samples were subsequently tested as three-point bending test with a cross speed of 1 mm/min at 25 °C and 1600 °C under argon. In addition, creep under variable stress was carried out at 1600 °C also under argon. The bending was reported as loading point displacement and not as the real bending strain because the elastic deformation of the apparatus, especially at high temperatures, affects the interpretation of the results. However, a calculated value of samples' fracture strain is given in Table 2 for comparison purposes. The creep tests were performed using bending tests with stress-increasing steps. The starting stress was about 70% of the value of high-temperature bending strength of the samples. The loading increased in several steps up to the fracture of the samples. For creep tests the displacement was plotted vs. time.

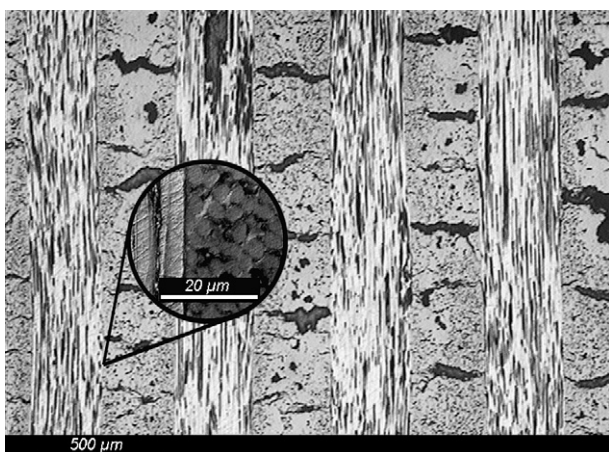


Fig. 1. Woven structure of C/C preforms (SEM, BS).



Fig. 2. Random orientation of uncoated fibers in felts (SEM, SE).

Table 2
Three-point bending strength and strain of the infiltrated sample at 25 °C and 1600 °C

Preform + matrix	Property			
	Tested at 25 °C		Tested at 1600 °C	
	Bending strength ^a (MPa)	Bending strain ^b (%)	Bending strength ^a (MPa)	Bending strain ^b (%)
C/C + MoSiTi (CM)	199 ± 3	0.63 ± 0.02	244	0.69
C/C + Si (CS)	206 ± 19	0.7 ± 0.04	246	1.19
Felt + MoSiTi (FM)	150 ± 7	0.34 ± 0.02	85	0.61
Felt + Si (FS)	123 ± 4	0.38 ± 0.01	56	0.52

^a Three measurements at 25 °C, one measurement at 1600 °C.

^b The strain values include the strain of apparatus and therefore can be used only for comparison.

3. Results and discussion

The alloy-infiltrated C/C composite obtained at 1550 °C had two quite different microstructures in its outer and inner parts. While in the fully infiltrated outer parts all the individual fibers were surrounded by solidified melt (Fig. 3a), only larger pores between fiber bundles got infiltrated in the inner parts (Fig. 3b). In the outer parts, the amorphous carbon in the matrix reacted with silicon from the melt and produced a SiC layer around the fibers (Fig. 3c). Apart from SiC, the matrix also included MoSi₂, which was found in the former large pores (Fig. 3d) and a solid solution of Mo and Ti silicides as well. Chemical composition of this solid solution was showed to be (Ti_{0.8}, Mo_{0.2})

Si₂ through XRD analyses. No residual silicon was observed in this composite (see also refs. 17,18).

The developed SiC layer acts as a melt penetration barrier and retards the next infiltration steps and the diffusion of silicon atoms via SiC layer dominates the kinetic of infiltration.¹⁹ Moreover, as the silicon reacts with carbon, the viscosity of the melt increases on its way into the inner parts. This raises the melting temperature of the melt and causes it to solidify before penetrating into the bundles in the inner parts.

The felts got fully infiltrated with MoSiTi at 1550 °C (Fig. 4). The carbon fibers reacted at their surfaces with silicon to form SiC. They remained non-reacted in their inner parts. SiC, MoSi₂ and TiSi₂ were the main phases in the matrix after infiltration.

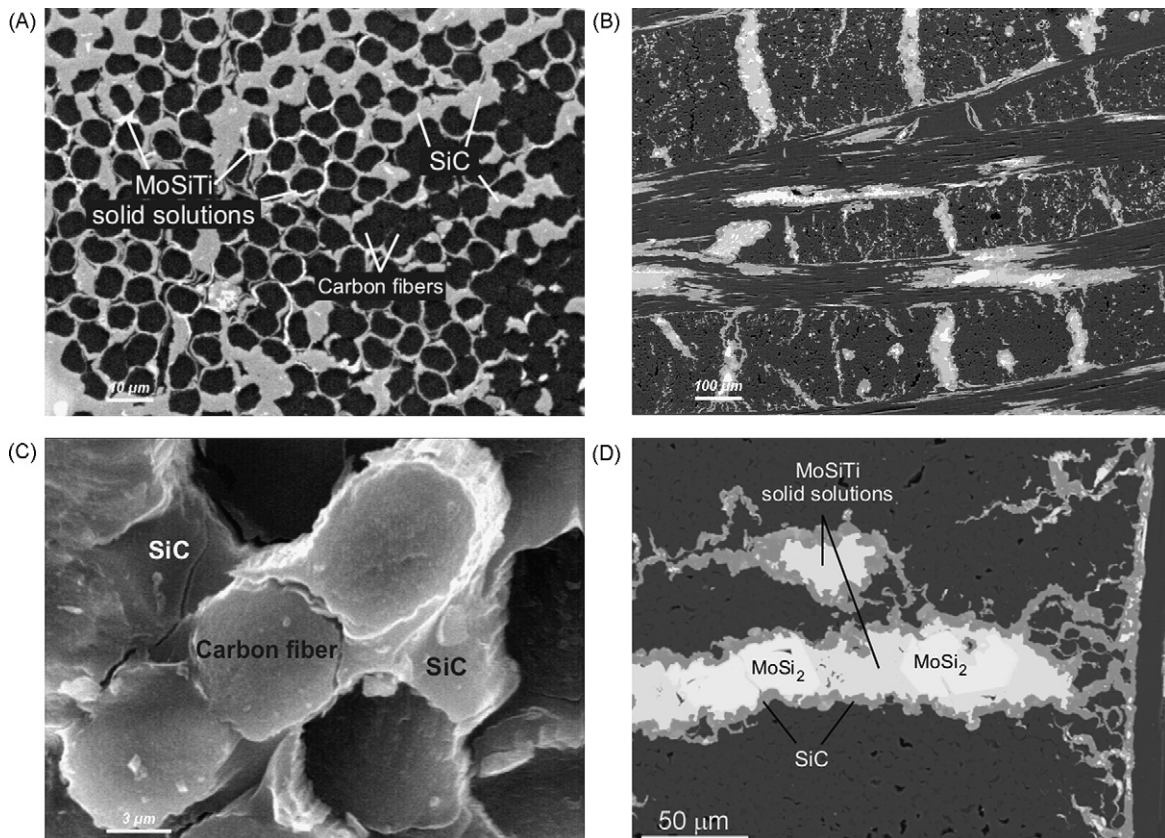


Fig. 3. Microstructure of infiltrated C/C samples; (a) fully infiltrated outer parts (SEM, BS), (b) partially infiltrated inner parts (SEM, BS), (c) thin SiC layer around the fibers (SEM, SE), (d) large MoSi₂ zones in the large capillary pores after infiltration (SEM, BS).

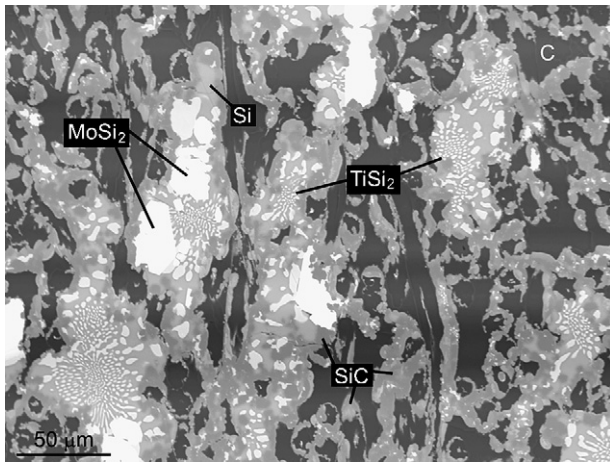


Fig. 4. Monolithic microstructure of infiltrated felts (SEM, BS).

Only little amount of free silicon was found in the infiltrated felts. This amount of free silicon in the sample could not diffuse through the developed SiC layer and react with the carbon in the short infiltration time which was given.

Through infiltration of MoSiTi and silicon melts into C/Cs and felts, four groups of samples (CM, CS, FM, and FS) were prepared. The values of ultimate bending strength and strain

(included strain of the apparatus) measured on each composite are summarized in Table 2. The reported room-temperature strength is a mean value of three measurements, while only one measurement at 1600 °C could be performed. Moreover, since the compliance of the test apparatus affects the measured data, it was not possible to calculate the Young's modulus from the bending curves.

It can be seen that the bending strength of the C/C composites is higher than the felt composites both at room-temperature and at 1600 °C. This is a result of reinforcing with high strength carbon fibers which can bridge the cracks and the longitudinal yarns which support the loading. Especially in the C/C composites with high volume fraction of fibers, the strength of the composite is strongly dependent on the fibers which possess higher strength values than the matrix phases.²⁰ Since both the CM and CS composites contained the same fibers with the same volume fraction, there was no considerable difference between their mechanical behaviors. Both of these composites underwent a rupture at an applied stress of about 200 MPa while the loading point was displaced about 0.2–0.3 mm at 25 °C (Fig. 5(a)). No catastrophic failure was observed in both cases. Small differences in the rigidity can be related to the matrix phases and their interfaces with the fibers.²¹ Stress–displacement curves for infiltrated felts at 25 °C are shown in Fig. 5(b). The composites showed brittle behavior and catastrophic failure. The FM com-

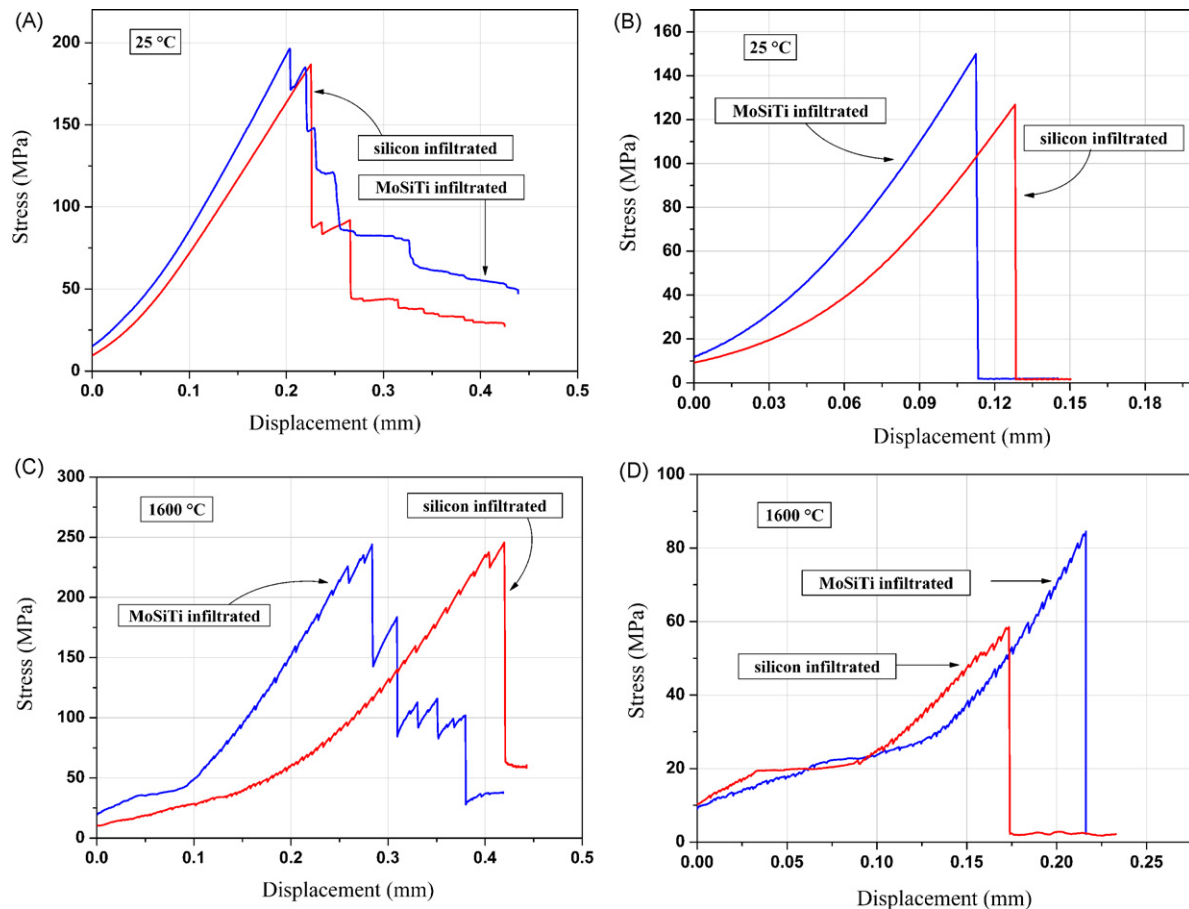


Fig. 5. Room-temperature stress–displacement curves of MoSiTi infiltrated and silicon-infiltrated composites (a) developed at 25 °C using C/C preforms, (b) developed at 25 °C using felt preforms, (c) developed at 1600 °C using C/C preforms, (d): developed at 1600 °C using felt preforms.

posite had a higher strength which, among other microstructural reasons, can be due to its different phases.

At 1600 °C the strength of infiltrated C/C composites increased (Fig. 5(c)). This is due to an increase of fiber strength with increasing temperature. Such an increase in the strength of different C/C composites which was also observed by other authors^{22,23} is a characteristic property of carbon fibers. At 1600 °C both of these composites showed higher values of displacement in comparison to room-temperature. More deformation of the CM sample is due to the increase in ductility of MoSi₂ at high temperatures. Large increase in the deformation of CS sample is caused by partially melting of the matrix phases.

Due to the softening of the residual silicon, the bending strength of the infiltrated felts fell at 1600 °C (Fig. 5(d)). However, it is important to notice that the bending strength of FM was consistently higher than FS. SEM analysis revealed grain growth and recrystallization processes in the microstructure of FM after heat treatment at 1600 °C. Crystallization of secondary micro-fibers and also growth of primary crystals help this composite withstand higher applied stresses. If the residual silicon in FM can be removed through optimizing the infiltration time and temperature, this composite can be favorable high-temperature applications. An increase in infiltration time and/or temperature could help processing silicon-free felt composites. Unfortunately such long-time infiltration tests could not be included in this work.

As described before, the creep tests were performed using bending tests with stress-increasing steps. The tests were performed with the same apparatus and under the same conditions as bending tests. The starting stress was about 180 MPa for CM and CS, 50 MPa for FM, and 40 MPa for FS. Fig. 6(a) shows the creep of CM at constant temperature of 1600 °C. The loading point was displaced 0.2 mm during the loading process. A primary creep stage was detected after loading. The deformation rate decreased and reached a value of about zero at the end of this primary stage. The second loading step was applied before stationary creep can be observed in the first step. After starting the second loading step, primary creep was again observed. This short-time primary creep led to fracture after some minutes. The CM sample showed only marginal creep deformation. This behavior is very similar to that observed by other authors and supports the suggestion that the initial creep occurs because of load-sharing effects, after which only marginal creep strain occurs.^{24–27} It also implies that a damage mechanism controls the creep of C/C composites. After the saturation of matrix-cracking in the first stage of creep, the creep of composite is controlled by a combination of the energy dissipative mechanisms like fiber debonding, fracture and pull-out of the fibers, matrix microcracking, etc.²⁸

The CM sample underwent failure at about 190 MPa which was near to its room-temperature strength (Fig. 6(a)). It can be expected that under creep conditions and because some thermally activated damage processes, many imperfections and

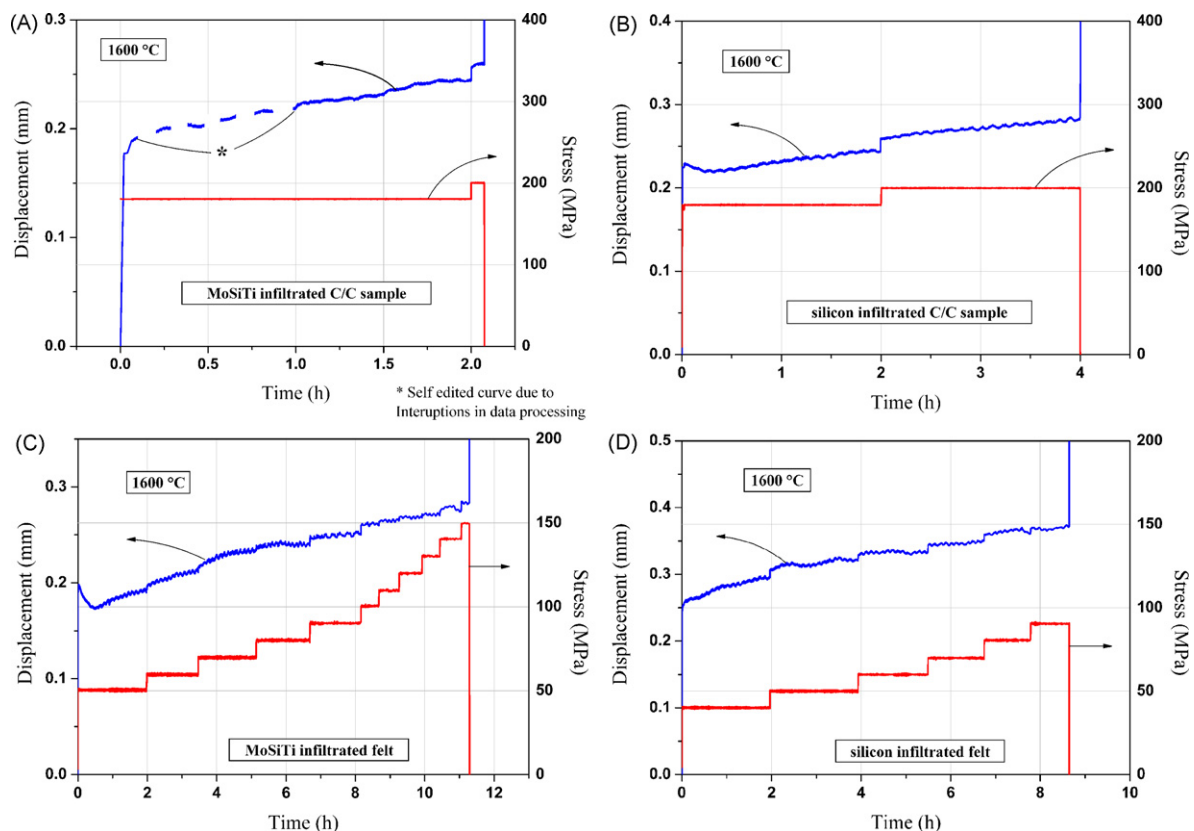


Fig. 6. Creep of different infiltrated samples at 1600 °C under argon atmosphere; (a) MoSiTi infiltrated C/C, (b) silicon-infiltrated C/C, (c) MoSiTi infiltrated felt, (d) silicon-infiltrated felt.

defects develop in the microstructure. Consequently the composite never reach its fast fracture strength. Moreover, the initial creep loading results in matrix-cracking, which leads to acceleration of the rupture process.²⁵

The creep of CS samples is demonstrated in Fig. 6(b). CS showed similar creep deformation to CM. This similarity implies again the dominating role of the fibers in mechanical properties of C/C composites and the creep behavior of CS can be explained by the same arguments as for the CM.

Although the CS samples could withstand the applied stress longer than CM samples, both of the samples broke under the same applied stresses of 200 MPa. Actually the ultimate stress at which the samples break is depending only on the fibers which are the same in both cases. The difference in the time-to-failure parameter is due to the distribution and the frequency of the microstructural defects and microcracks which lead to the creation of main cracks, the master crack, and finally to the rupture of the composite.

As it can be seen in Fig. 6(c and d), the FM and FS samples broke under creep conditions finally at applied stresses of 150 MPa and 100 MPa, respectively. These values of stress are much higher than the ultimate bending strength of the samples measured at 1600 °C. In order to explain this result it is necessary to recall the problems in analyzing creep curves which are obtained from bending tests. In Fig. 7 it could be seen that the longitudinal stresses in the specimen vary with the distance from the neutral axis.^{29,30} This means the real-time stress which develops locally inside the sample during creep is not necessarily equal to the stress which calculated based on linear-elastic behavior. Although a constant load is applied over a long-time, the points with different distances from the neutral axis are exposed to different tensile or compression stresses. These stress variations depend on the parameter n , the stress exponent for creep. In the case of $n=1$ the initial linear stress distribution over the specimen cross-section remains constant and linear also during creep. However, if the stress exponent gets higher values ($n > 1$), the outer regions of the bending creep specimen tend to creep faster compared to the linear-elastic case and the creep law

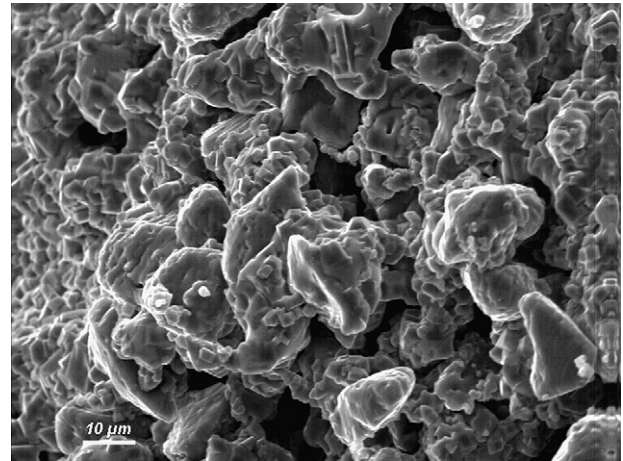


Fig. 8. Microstructure of creep tested MoSiTi infiltrated felt (SEM, SE).

with $n = 1$ (see Fig. 7). This results in stress relaxation and stress redistribution in these regions. Due to these ongoing stress relaxations in the outer regions of the bending specimen during creep, the specimen can withstand higher applied loads in the following loading steps up to final fracture stress level. This effect is more pronounced if the sample shows a higher plasticity at high temperatures and that is the case for the infiltrated felts in which the plasticity of the phases increases considerably at 1600 °C.

Changes in the microstructure of the felt composites are other reasons for the increase in their strength under creep conditions. The microstructure of creep tested FM is shown in Fig. 8. After about 10 h heat treatment at 1600 °C two main changes can be seen compared to the situation before the heat treatment. First, there are more pores in the microstructure; and second, the grains bonded together and formed large aggregates. No free silicon could be detected in the microstructure of this creep tested sample using semi-quantitative chemical analysis. Silicon has seemingly reacted further with other elements in the composite to form more silicide or carbide grains. This means it is possible to develop silicon-free felt composites as well (silicon-free C/C composites were already obtained in this work) by increasing the infiltration time.

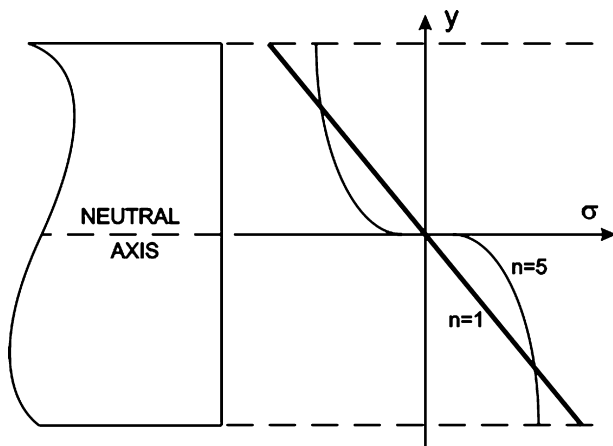


Fig. 7. Variation of the longitudinal stresses with distance from the neutral axis in a 4-point bending-beam as a function of n , the stress exponent parameter, according to ref. ²⁸

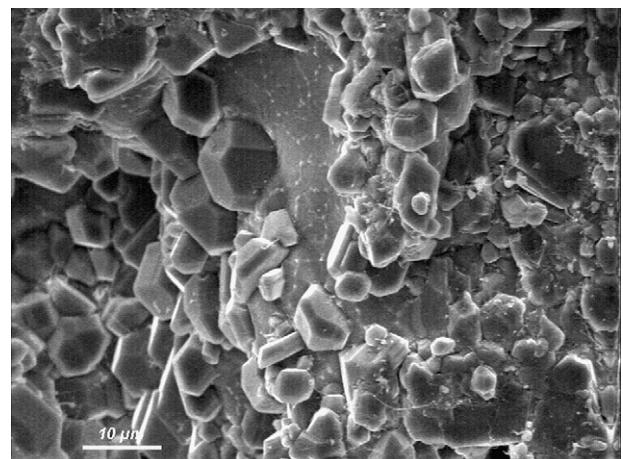


Fig. 9. Microstructure of creep tested silicon-infiltrated felt (SEM, SE).

In the case of creep tested FS, rather large pores in the microstructure caused a rough fracture surface on which coarse SiC crystals was observed (Fig. 9). SiC crystals which were formed by the reaction between silicon and carbon during infiltration grew to make larger crystals. The silicon from the matrix reacted further with carbon leading either to SiC in form of new crystals or to growth of the primary crystals.

Channel-formed large pores in the microstructure (Fig. 9) can result from flowing of silicon out of the sample after its melting or evaporating. Although such large pores in the microstructure of both samples can cause the ultimate strength to decrease, but the remaining porous material, especially in case of FM, has strong bonding between its grains which helps the composite withstand higher applied stresses as it was proposed.

4. Conclusion

Carbon fiber preforms were infiltrated with an alloyed melt of Si, Ti and MoSi₂ at temperatures below 1600 °C. SiC, MoSi₂ and a solid solution with the chemical composition of (Ti_{0.8}, Mo_{0.2}) Si₂ were the main phases in alloy-infiltrated C/C samples. Under optimized conditions C/C composites without residual silicon can be obtained. No free silicon was detected in alloy-infiltrated C/C composites by SEM studies. The fibers in C/C preforms showed no severe reaction with the melt. They controlled the mechanical properties of C/C composites. At 1600 °C, these composites exhibited only marginal creep deformation and their bending strength was even better than at room-temperature. But we must recall that only one test was performed at 1600 °C.

The felts were fully infiltrated with MoSiTi and formed a monolithic composite. As well as SiC, there were MoSi₂, TiSi₂, non-reacted carbon and little amount of free silicon in the microstructure of these composites. In infiltrated felts the matrix phases dominated the mechanical properties. Grain growth and recrystallization processes were observed in the microstructure of these samples which seemed to be favorable for high-temperature applications; however, the presence of residual silicon reduced their high-temperature strength. A silicon-free felt composite could be obtained through optimization of time and temperature of the infiltration, which could not be included in this work. The felt composites underwent more creep deformation than C/C composites and showed changes in their microstructure under creep conditions.

Acknowledgements

Special thanks to the AiF (Germany) for their supports to the project 13411N.

References

- Hillig, W. B., Mehan, R. L., Morelock, C. R., Dicarolo, V. J. and Laskow, W., Silicon–silicon composites. *Gen. Electr. Rep.*, 1974, **74**(November), CRD 282.
- Hillig, W. B., Properties and structure of melt infiltrated composites. *Ceram. Eng. Sci. Proc.*, 1988, **9**, 755–758.
- Larsen, D. C., Adams, J., Johnson, L., Teotia, A. and Hill, L., *Ceramic materials for heat engines*. Noyes Publication, NY, 1985.
- Gadow, R. and Fitzer, E., Fiber-reinforced silicon carbide. *Am. Ceram. Soc. Bull.*, 1986, **65**(2), 326–335.
- Forrest, C. W., Kennedy, P. and Shennan, J. V., The fabrication and properties of self-bonded silicon carbide bodies. In *Special ceramics*, ed. P. Popper. 5 ed. The British Ceramic Research Association, Stoke on Trent, 1972, pp. 99–123.
- Trantina, G. G. and Mehan, R. L., High-temperature time-dependent strength of a Si/SiC composite. *J. Am. Ceram. Soc.*, 1977, **60**(3–4), 177–178.
- Singh, M. and Dickerson, R. M., Characterisation of SiC fiber (SCS-6) reinforced-reaction-formed silicon carbide matrix composites. *J. Mater. Res.*, 1996, **11**(3), 746–751.
- Meier, S. and Heinrich, J. G., Processing-microstructure-properties relationships of MoSi₂–SiC composites. *J. Eur. Ceram. Soc.*, 2002, **22**, 2357–2363.
- Messner, R. P. and Chiang, Y. M., Liquid-phase reaction-bonding of silicon carbide using alloyed silicon-molybdenum melts. *J. Am. Ceram. Soc.*, 1990, **73**(5), 1193–1200.
- Henager, C. H., Brimhall, J. L. and Hirth, J. P., Synthesis of a MoSi₂–SiC composite *in situ* using a solid state displacement reaction. *Mater. Sci. Eng.*, 1992, **A155**, 109–114.
- Jeng, Y. L. and Laverina, E. J., Review processing of molybdenum disilicide. *J. Mater. Sci.*, 1994, **29**, 2557–2571.
- Petrovic, J. J. and Honnel, R. E., MoSi₂ particle reinforced-SiC and Si₃N₄ matrix composites. *Mater. Sci. Lett.*, 1990, **9**, 1083–1084.
- Gac, F. D. and Petrovic, J. J., Feasibility of a composite of SiC whiskers in an MoSi₂ matrix. *J. Am. Ceram. Soc.*, 1985, **68**(8), C200–C201.
- Carter, D. H. and Hurley, G. F., Crack deflection as a toughening mechanism in SiC-whisker reinforced MoSi₂. *J. Am. Ceram. Soc.*, 1987, **70**(4), C79–C81.
- Lowden, R. A. and More, K. L., The effect of fiber coatings on interfacial shear strength and the mechanical behavior of ceramic composites. In *Mat. Res. Soc. Symp. Proc., Interfaces in Composites*, ed. C. G. Pantano and E. J. H. Chen, 1990, p. 205.
- Kerans, R. T., Hay, R. S., Pagano, N. J. and Parthasarthy, T. A., The role of the fiber-matrix interface in ceramic composites. *Am. Ceram. Soc. Bull.*, 1989, **68**, 429–442.
- Esfahanian, M., Development of high temperature carbon–silicide–carbide composites via reactive melt infiltration, Ph.D. Thesis. Clausthal University of Technology, ISBN: 3183724057, Fortschritt-Berichte 5,724, VDI-Verlag, Düsseldorf, 2006.
- Esfahanian, M., Günster, J., Moztarzadeh, F. and Heinrich, J. G., Development of a high temperature C_f/XSi₂–SiC (X = Mo, Ti) composite via reactive melt infiltration. *J. Eur. Ceram. Soc.*, 2007, **27**, 1229–1235.
- Heidenrich, B., Manufacturing of fiber reinforced ceramics using liquid silicon infiltration (LSI-Technik). In *Ceramic composites*, ed. W. Krenkel. Wiley-VCH, Weinheim, 2003, pp. 48–75.
- Zok, F. W., Evans, A. G. and Mckin, T. J., Theory of fiber reinforcement. In *Handbook on continuous fiber reinforced ceramic matrix composites*, ed. R. L. Lehman, S. K. El-Rahaiby and J. B. Wachtman. Purdue University and American Ceramic Society, 1996, pp. 35–110.
- Kerans, R. J., Hay, R. S. and Pagano, N. J., The role of the fiber–matrix interface in ceramic composites. *Am. Ceram. Soc. Bull.*, 1989, **68**(2), 429–442.
- Thomas, C. R., What are carbon–carbon composites and what do they offer. In *Essentials of carbon–carbon composites*, ed. C. R. Thomas. The Royal Society of Chemistry, Cambridge, 1993, pp. 1–36.
- Mc Enaney, B. and Mays, T., Relationship between microstructure and mechanical properties in carbon–carbon composites. In *Essentials of carbon–carbon composites*, ed. C. R. Thomas. The Royal Society of Chemistry, Cambridge, 1993, pp. 143–173.
- Darzens, S., Chermant, J.-L., Vicens, J. and Sangleboeuf, J.-C., Understanding of the creep behavior of SiC_f–SiBC composites. *Scripta Mater.*, 2002, **47**, 433–439.
- Boitier, G., Darzens, S., Chermant, J.-L. and Vicens, J., Microstructural investigation of interfaces in CMC composites. *Composites*, 2002, **A33**, 1467–1470.
- Chermant, J.-L., Boitier, G., Darzens, S., Farizy, G., Vicens, J. and Sangleboeuf, J.-C., The creep mechanism of ceramic matrix composites at low temperatures and stress by a material science approach. *J. Eur. Ceram. Soc.*, 2002, **22**, 2443–2460.

27. Lee, S. S., Zawada, L. P., Staehler, J. M. and Folsom, C. A., Mechanical behavior and high-temperature performance of a woven NicalonTM/Si-N-C ceramic–matrix composite. *J. Am. Ceram. Soc.*, 1998, **81**(7), 1797–1811.
28. Ladevèze, P., On an anisotropic damage theory. In *Failure criteria of structured media*, ed. J. P. Boehler. Blakena, Rotterdam, 1993, pp. 355–363.
29. Becher, P. F. and Francis Rose, R., Toughening mechanisms in ceramic systems. In *Materials science and technology; a comprehensive treatment*, vol. 11. In *Structure and properties of ceramics*, vol. ed., ed. R. W. Cahn, P. Haasen and E. J. Kramer. Swain M.V., VCH publishers Inc., Weinheim, 1994, pp. 410–458.
30. Cohrt, H., Grathwohl, G. and Thuemmler, F., Non-stationary stress distribution in a ceramic bending beam during constant load creep. *Res. Mech.*, 1984, **10**, 55–71.